

Calibration of the forward and rear ZEUS calorimeter using cosmic ray muons

U. Behrens ^{a,1}, G. Cases ^b, A. Freidhof ^c, A. Fürtjes ^{d,2}, J. Mitchell ^{e,3}, K. Molthagen ^f,
B. Surrow ^d, T. Tsurugai ^d, R. Yoshida ^{g,4,*}

^a *I. Institut für Experimentalphysik, Universität Hamburg, Hamburg, Germany*

^b *Universidad Autónoma de Madrid, Spain*

^c *Universität Freiburg, Germany*

^d *DESY, Hamburg, Germany*

^e *McGill University, Canada*

^f *II. Institut für Experimentalphysik, Universität Hamburg, Hamburg, Germany*

^g *NIKHEF-H, Amsterdam, The Netherlands*

(Received 13 September 1993)

The forward and rear calorimeter of the ZEUS experiment consists of 48 modules. Before their installation into the ZEUS detector they were calibrated at DESY using cosmic ray muons in order to check their performance and to compare the response to cosmic muons to the response, obtained for some modules, to 100 GeV beam muons. The setup, the test procedure and the analysis of the data are described in this paper. The relative calibration of the different modules, as well as of the different cells within a module can be obtained with cosmic ray muons with an accuracy of about one percent for a measurement time of 3–5 days/module.

1. Introduction

The central component of the ZEUS detector at the e–p collider HERA at DESY is the high resolution calorimeter. It is built of depleted uranium plates as absorber and plastic scintillator tiles as active medium. The forward (FCAL) and rear (RCAL) calorimeter consists of 48 modules.

The detailed performance of the calorimeter has been optimized and measured using a prototype. In the energy range between 10 and 100 GeV an energy resolution of $(34.9 \pm 0.3\%)/\sqrt{E}$ for hadrons, $(18.0 \pm 0.3\%)/\sqrt{E}$ (E in GeV) for electrons and an electron to hadron response of $e/h = 1.00 \pm 0.01$ has been achieved [4]. For sufficiently high energy deposits (more than 1 GeV) a time resolution in the subnanosecond region was measured.

Equally important as its energy resolution is the absolute energy calibration of the calorimeter. The following methods are employed to achieve the 1% calibration accuracy required:

- tight quality control of mechanical dimensions and the uniformity of the optical components [2],
- scans with a pointlike ⁶⁰Co-source along the scintillators of each calorimeter cell to verify the uniformity of the response of the scintillators and wavelength shifters [5],
- calibration of the readout electronics [2,24],
- relative calibration of all cells using the signal from the uranium radioactivity,
- beam calibration of a prototype calorimeter of identical construction to the final calorimeter modules to relate the absolute energy deposit of different particles (hadrons, electrons and muons) to the uranium signal [4,1],
- light-injection (LED and LASER) calibration to determine the linearity of the readout system [16,3],
- beam calibration of final calorimeter modules to verify the accuracy of the uranium calibration. This has been done during 1989 and 1990 for six modules of the forward calorimeter and four modules of the rear calorimeter at the CERN SPS and an agreement be-

* Corresponding author.

¹ Now at DESY, Hamburg, Germany.

² Now at II. Institut für Experimentalphysik, Universität Hamburg, Germany.

³ Now at CERN, Geneva, Switzerland.

⁴ Now at H.H. Wills Physics Laboratory, University of Bristol, UK.

tween beam and uranium signal calibration within 1% has been achieved [2],

– cosmic ray calibration of (nearly) all of the forward and rear calorimeter modules at DESY as a final check before the installation into ZEUS and as a verification of the accuracy of the uranium calibration for all modules. This last test was performed during 1990 and 1991 and is the topic of this paper.

Since March 1992 all calorimeter modules are operational in the ZEUS detector and data from e–p collisions have been taken since June 1992.

2. The ZEUS calorimeter

The ZEUS calorimeter is described in detail in ref. [28]. It surrounds the solenoid and tracking detectors. The calorimeter is divided into three main components:

– Forward CALorimeter (FCAL) covering polar angles from $\theta = 2.2^\circ$ to 39.9° (measured from the p-beam direction).

– Barrel CALorimeter (BCAL) extending from $\theta = 36.7^\circ$ to 129.2° .

– Rear CALorimeter (RCAL) between $\theta = 128.1^\circ$ and 176.5° .

The calorimeter consists of a sampling structure using depleted uranium as absorber and scintillator as active medium with a sampling step of one radiation length (X_0) throughout. Longitudinally the readout is subdivided into two parts. The part closest to the interaction point forms the electromagnetic calorimeter (EMC) with a depth of about $25X_0$, or 1.0 interaction length (λ). The remainder forms the hadronic calorimeter (HAC). Its depth varies with the polar angle, in the FCAL from 6.2λ to 4.6λ , in the RCAL from 3.1λ to 2.3λ , and 3.9λ in the barrel. The EMC part is read out as one section in depth. For FCAL and BCAL the HAC is divided further into two sections, HAC1 and HAC2. RCAL has only one HAC section. Transversally the calorimeter is segmented in towers. The planes of divisions are nonprojective for FCAL and RCAL. For BCAL, both EMC and HAC are projective in azimuthal angle but only the EMC is projective in θ . The central part of the FCAL (RCAL) have EMC cells with dimensions of $5 \times 20 \text{ cm}^2$ ($10 \times 20 \text{ cm}^2$). In the outer regions where the cells are shadowed by the BCAL the segmentation is $20 \times 20 \text{ cm}^2$.

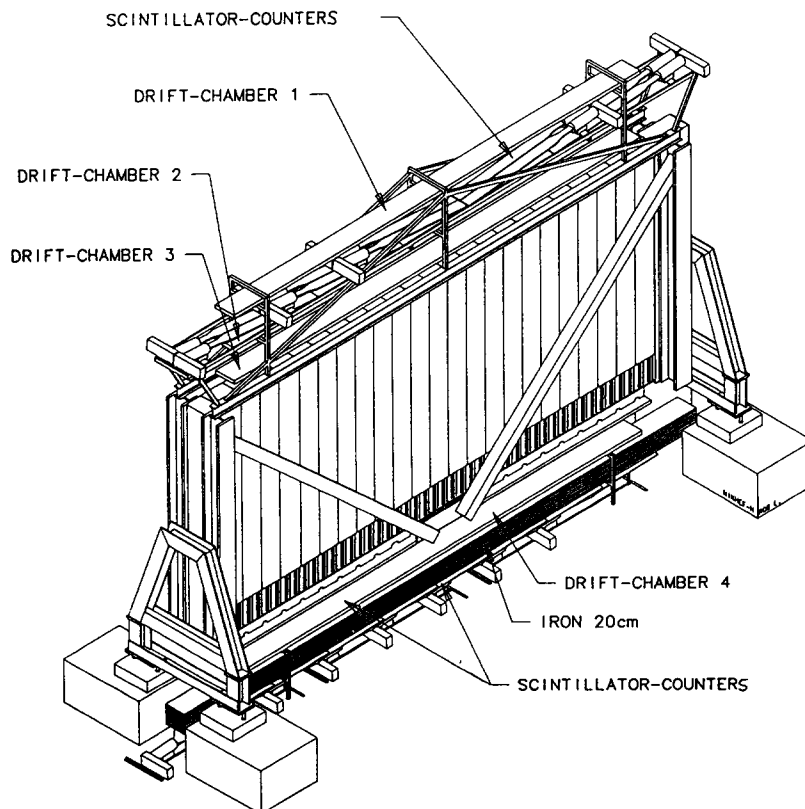


Fig. 1. Setup of the cosmic ray test stand in DESY hall II.

These cells are called HAC0. In the BCAL the EMC segmentation is $4.9 \times 23.3 \text{ cm}^2$. The granularity in the hadronic calorimeter is $20 \times 20 \text{ cm}^2$ in F/RCAL and $24.4 \times 27.1 \text{ cm}^2$ for BCAL calorimeter.

The size and weight of the calorimeter make modular construction and installation necessary. FCAL and RCAL consist of 24 modules each including 2 special half-sized modules positioned above and below the beam pipe.

The F/RCAL modules have heights between 2.2 and 4.6 m and depths between 70 and 152 cm in their active area depending on their position with respect to the beam. The width of the modules is 20 cm. The surface towards the interaction point of the assembled modules of FCAL and RCAL approximate a circle of 230 cm radius. A detailed description of the different calorimeter modules can be found in refs. [6,2,28].

3. Experimental setup

3.1. Description of the test stand

The cosmic ray test stand was located in the DESY experimental hall II. The setup is shown in Fig. 1. It consisted of a movable upper frame with scintillation trigger counters and drift chambers which were placed on top of the calorimeter module to be tested. The calorimeter module itself was orientated in the so-called stacking position with the surface that would face the interaction point upwards. Below the module a 10 cm thick iron absorber, a frame with scintillation counters and another drift chamber were placed. The different components of the setup will now be described in more detail.

3.1.1. Scintillation counters

Three layers of scintillation counters were used in the trigger system. One layer was located above and the other two below the calorimeter module. Between the two layers of the bottom trigger system a 10 cm thick iron absorber was inserted in order to ensure a minimum muon energy.

The upper trigger layer consisted of ten counters (u1l, u1r, ..., u5l, u5r) with a size of $8.0 \times 90.7 \text{ cm}^2$ each. They were placed as five pairs with a gap of 1.0 cm in order to resolve the ambiguity of the drift chamber position reconstruction. Along the module the counters overlapped by about 1 cm. For layer two, five counters (m1, ..., m5) with a size of $25.8 \times 101.5 \text{ cm}^2$ each were used. The overlap was about 5 cm. The bottom layer consisted of 8 scintillation counters (d1, ..., d8) of $20.0 \times 60.0 \text{ cm}^2$ each. These scintillators overlapped by about 1 cm. All scintillation counters were equipped with photomultipliers of the type Valvo 56AVP and Cockcroft–Walton bases for the high voltage supply.

Using a ruthenium source the dependence of the trigger efficiency on the high voltage was measured for each individual counter. A voltage at the beginning of the observed plateau was then chosen to operate the scintillators with efficiencies larger than 99%. The voltages were between 1600 and 2100 V for discriminator thresholds of 50 mV.

For data taking with shorter modules an additional counter was used to veto triggers for muons missing the calorimeter module.

3.1.2. Drift chambers

To measure the muon track, four drift chambers of the DELPHI muon end cap type [12] with an active

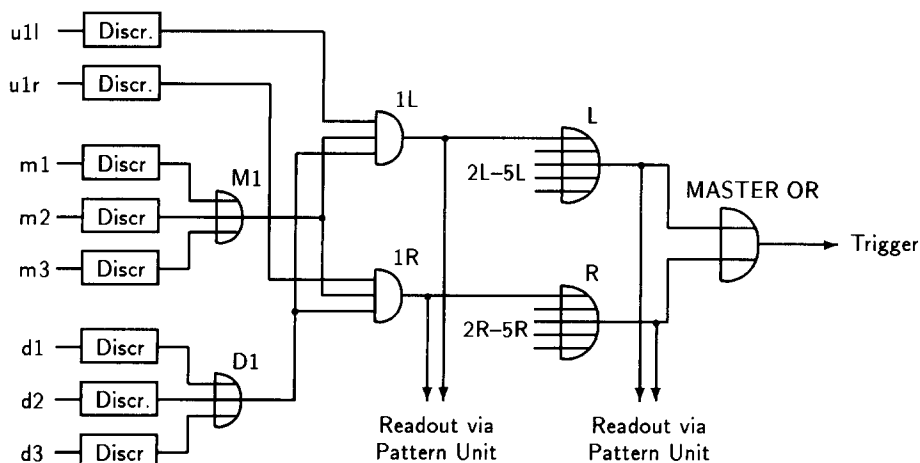


Fig. 2. Layout of the fast trigger electronics.

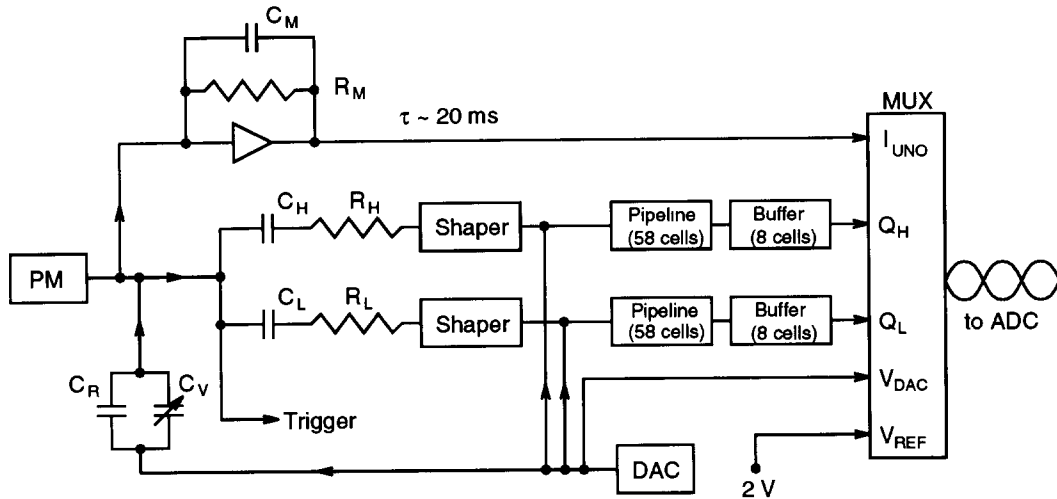


Fig. 3. Schematic layout of a front-end card.

size of $428 \times 18.8 \text{ cm}^2$ were used. Three of them were positioned above and one below the module. The chambers at the top were separated by 30 cm and the third one located 26 cm above the module. The chamber below the module was placed on top of the iron absorber, 30 cm below the module's end plate. The chambers were operated in the limited streamer mode, using a 50–50 Ar–CO₂ gas mixture with a small addition of isopropanol as a quencher [25,26]. They had one central anode wire and a delay line along their length, each chamber therefore had only three readout channels to reconstruct the position of a muon.

Due to the gas mixture the maximum reconstruction efficiency obtained for a muon track above the calorimeter module was only $20 \pm 5\%$. The position resolution could be determined to be 3.8 mm along the chamber and 1.2 mm in drift direction. Further details can be found in ref. [18]. In the analysis it was found that adequate reconstruction of tracks could be achieved by the calorimeter alone; the drift chambers were only used for specific studies.

3.1.3. Trigger

The logic of the fast trigger for one out of five trigger sections ^{#1} is shown in Fig. 2. The trigger rate was 0.22 s^{-1} per trigger section for FCAL and 0.41 s^{-1} per trigger section for RCAL. The minimum energy of a muon passing through the calorimeter stack producing a trigger signal is about 1.7 GeV for FCAL and 1.1 GeV for RCAL.

^{#1} With trigger section we describe a pair of top counters in coincidence with the corresponding bottom counters (e.g. 1L and 1R together) (see Fig. 2).

The muon flux at sea level for the so called “hard component” ($E_\mu > 0.2 \text{ GeV}$) is given in refs. [21,23] as $80 \text{ m}^{-2} \text{ s}^{-1} \text{ sr}^{-1}$. From an integral range spectrum of muons at sea level given in [23] one extracts for the muon flux $41 \pm 1 \text{ m}^{-2} \text{ s}^{-1} \text{ sr}^{-1}$ for FCAL and $53 \pm 1 \text{ m}^{-2} \text{ s}^{-1} \text{ sr}^{-1}$ for RCAL. With a solid angle acceptance of $0.04 \pm 0.005 \text{ sr}$ for FCAL and $0.06 \pm 0.005 \text{ sr}$ for RCAL the predicted trigger rate is $0.24 \pm 0.04 \text{ s}^{-1}$ per trigger section for FCAL and $0.46 \pm 0.005 \text{ s}^{-1}$ per trigger section for RCAL. This is in agreement with the measured rates.

3.2. High voltage supply

The high voltage supply for the photomultipliers uses miniature Cockcroft–Walton HV bases ^{#2} mounted directly on the phototube. The photomultipliers and the Cockcroft–Walton supplies of the ZEUS forward and rear calorimeter are described in ref. [20]. The high voltage can be set with an accuracy of about 0.5 V. The temperature dependence of the high voltage is $0.025\%/^{\circ}\text{C}$, and the ripple of the cathode voltage at -1800 V is 0.4 V [14].

Prototypes of the 36 channel ZEUS VME HV controller were used to set, control and read back the high voltage.

3.3. Readout electronics

The signals from the PMs were read out with the same electronics as in the ZEUS experiment [24]. The

^{#2} Model HPMC-1.8N and HPMC-2.2N fabricated by Matsusada Precision Dev. Inc.

readout is done in two steps: analog storage of the signals and digitization.

3.3.1. Analog electronics

The PM signals are sent via a 2 m coaxial cable to the shaping amplifiers which are located on front-end cards. The shaped pulse, which has a half width of about 100 ns, is sampled every 96 ns (the time between consecutive HERA bunches) by a 58 cell analog pipeline based on switched capacitor techniques [17]. The trigger stops the pipeline and the charge of the cells containing the signals is transferred to an analog buffer which again uses switched capacitor techniques. The signal is then sent via a multiplexer to the ADC. A schematic layout is given in Fig. 3. The front-end cards are mounted on the modules, and each card reads out 12 PM channels.

In order to cover the expected signal range at HERA (from 300 MeV for minimal ionizing particles up to 450 GeV of some hadronic final states) the PM signal is split into a “high gain” (Q_H) and a “low gain” (Q_L) path. Both paths are identical apart from a gain factor of 22.22. The high gain path covers the range between 0 and 20 GeV, while the low gain path is sensitive up to 450 GeV.

In addition the PM signal is split to measure the quasi dc current produced by the uranium radioactivity with a current to voltage converter using a feedback resistor with an integration time of 20 ms.

For the cosmic ray test the modules were equipped with the final FCAL front-end cards. These cards were mounted on a removable copper board so that the same set of cards were used to read out all the modules. The copper was cooled by water. In total 22 cards were used for the biggest module.

3.3.2. Digital cards

The analog signals from the front-end cards were transmitted via 60 m long flat twisted-pair cables to the digital cards, where they were digitized by 12-bit ADCs at a rate of 1 MHz. Every digital card contains 4 ADCs and processes the data from two front-end cards (24 channels). It incorporates a Motorola M56001 digital signal processor (DSP) that can calculate the energy and time information from the pulse samples. In the cosmic muon stand the DSP was only used to transfer the raw data. To read out the largest module 11 digital cards were needed. The cards are VME based and are read out by the NIKHEF 2TP-board which contains two INMOS T800 Transputers, 1 Mbyte private RAM and 128 kbyte dual ported RAM for VME access [7].

3.4. Data acquisition

The DAQ system consisted of four subsystems:

- A MicroVAX II with a 16 Mbyte RAM and 600 Mbyte disk space as host, interfaced to the fast trigger system, the CAMAC readout and the run-control.
- A 2TP-board to control the front-end cards, to read out the digital cards and to generate test triggers.
- CAMAC and NIM crates with the cosmic trigger logic and read out of the drift chambers, using 4208 LeCroy TDCs, and the trigger information.
- Slow control by a Motorola 68020 microprocessor running under OS9 driving the HV controllers.

Fig. 4 shows the scheme of the DAQ system. The transputers were connected to the MicroVAX by a 500 m long optical link and to the OS9 machine via Ethernet using TCP/IP. The readout tasks were implemented in the transputers. One of the transputers was used to control the front-end electronics, to react on

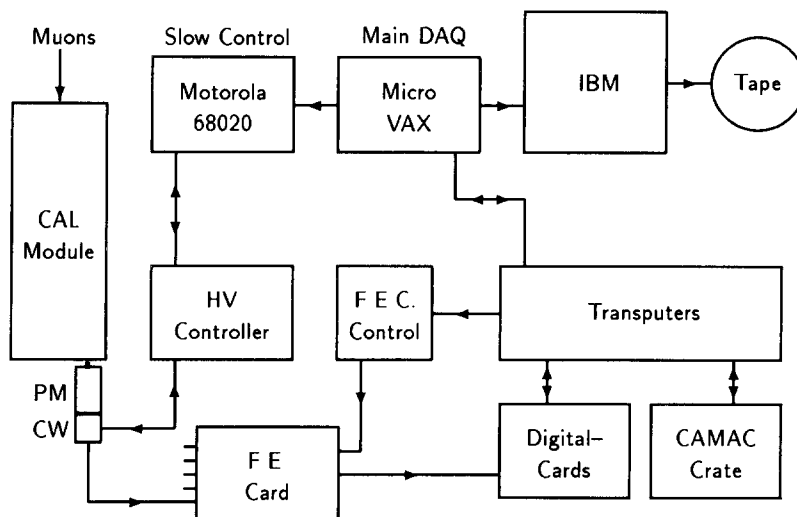


Fig. 4. Scheme of DAQ of the cosmic muon stand.

VME interrupts and to read out the VME-ADC and CAMAC crates. The data block was then transferred to the second transputer and was formatted into ZEBRA #³ banks. In order to reduce the amount of data, only the information from the “high-gain” path (see section 3.3) was kept for muon runs. The records obtained in this way were then buffered and transferred to the MicroVAX in blocks of 36 to 40 kbytes. The event data, as well as the data delivered by the CAMAC readout, were buffered in the MicroVAX using MBM #⁴ and were made available for storage on disk and data quality monitoring (DQM). The DQM was implemented using the PAW #⁵ package.

Data taking was controlled by a task implemented on the MicroVAX. This task could start, control and stop a run by sending commands to the transputers to set the trigger conditions for muons, UNO #⁶, LED #⁷, Laser or random triggers (PED). A run, formed by consecutive events with the same trigger condition, was stored as a single file on the VAX disk. In addition, a feature called “autopilot” was available to perform a sequence of runs with different parameters, such as trigger conditions or number of events.

The data were finally copied from the disk to the central IBM via the INTERLINK connection [20] and written to cartridges in the ZEBRA exchange format.

4. Test procedure

During the period from September 1990 to April 1991, 20 FCAL modules and 20 RCAL modules were tested in the cosmic ray stand. Only the small outer modules, which are covered by the BCAL in ZEUS, have not been tested due to the tight installation schedule of the ZEUS detector. These modules (4 FCAL and 4 RCAL) have only HAC0 towers. They represent only a few percent of all F/RCAL channels. In total 92.8% (91.7%) of FCAL (RCAL) channels were tested with cosmic muons.

Each module remained 3 to 5 days in the test stand. On average, 200 000 events (FCAL) and 300 000 events (RCAL) were recorded for every module.

#³ Data structure management system from the CERN ECP Division [8].

#⁴ Model Buffer Manager from the CERN ECP Division [27].

#⁵ Physics Analysis Workstation from CERN ECP Division [9].

#⁶ In an UNO-run the integrated signal from the radioactivity of the uranium is read out.

#⁷ In a LED/Laser-run the signal from the light injection by a LED or a Laser is read out.

4.1. Setting up

The preparation of one module for data taking consisted of the following steps:

- Installation and alignment of the module in the test stand.
- Installation of the upper trigger frame.
- Check of the trigger rate.
- Cabling and debugging of the HV of the PMs on the calorimeter.
- Cabling and debugging of the analog electronics.
- Repair of defective PMs.
- Search for light leaks. This was accomplished by setting the HV to 1000 V for all PMs and comparing the uranium signal (UNO) with the lights in the hall switched on and off. The difference was required to be less than 0.5%.

– Tuning of the HV of the PMs to reach the nominal UNO current values $I_{\text{UNO}}^{\text{nom}}$, with 1% precision. The values were:

- 100 nA for FEMC channels.
- 200 nA for REMC channels.
- 400 nA for FHAC0 and RHAC0 channels.
- 500 nA for FHAC1, FHAC2 and RHAC1 channels.

These values were chosen as the result of beam measurements with the FCAL prototype and the final FCAL and RCAL modules at CERN [4,2]. They result in a calibration for all channels of approximately 10 pC/GeV. These values are a compromise between noise, linearity of the response over the entire signal range, sufficiently large uranium current for accurate calibration and lifetime of the PMs [10].

The setting up took about 10 h in average.

4.2. Data taking

The data were taken in consecutive runs of 1000 events.

Regular UNO and PED measurements were performed. In the first 12 h of a test cycle, when the gains of the PMs were not yet stable, UNO runs were taken every hour. The HV values for the PMs were tuned again after 12 h. For the remaining period the uranium currents were measured every 8 h. Pedestal runs were performed every 8 h from the beginning.

Data quality monitoring was done every 8 h. The UNO values, the observed charge distribution and the number of muons per tower were checked.

At the end of a test cycle several runs to calibrate the front-end electronics were taken. Furthermore UNO pedestals and the electronics noise were measured at a HV of 400 V.

Finally, the upper trigger frame was removed and the module was prepared for transport to the ZEUS hall.

5. Analysis of the data

The time and charge reconstruction used during the analysis was identical to the one used for the analysis of the CERN beam test data of F/RCAL. The algorithms are described in detail in ref. [2].

5.1. Stability of calibrations and noise

For the reconstruction of the photomultiplier charge the analog electronics has to be calibrated and corrections for the different gains of phototubes and arrival times with respect to the 96 ns clock have to be applied. For this purpose 279 constants per channel plus 37 constants common to all channels are required. No update of these constants was necessary during the calibration of one module except the UNO current correction which was updated approximately every 8 h. After one week of running typical variations for the high gain readout path used for the muon measurements were 0.3% for the electronics gain, 0.03 pC for pedestals and 1.2% (0.7%) for UNO currents of EMC (HAC) channels. After 8 h of running the UNO current variations were typically 0.5% (0.2%) for EMC (HAC) cells.

The measured charge of 1 pC is approximately equivalent to 100 MeV of energy deposited by showers in the calorimeter.

The noise for individual channels has been determined with randomly triggered events. In the high gain channels it amounts to about 0.10 pC for FEMC and REMC, and 0.14 pC for FHAC0/1/2 and RHAC0/1 (see Fig. 5). This noise is dominated by the fluctuations of the uranium signal. The electronic contribution, determined by reducing the HV to 400 V, is 0.045 pC

(Fig. 5). The noise in the different calorimeter cells is uncorrelated, but the noise in right and left channels of the same cell is correlated by about 50% due to the uranium signal. The total noise in a $20 \times 20 \text{ cm}^2$ FCAL supertower (EMC + HAC1 + HAC2) adds up to about 0.42 pC corresponding to 44 MeV (high gain). The low gain channel, on the contrary, is dominated by electronic noise of about 0.80 pC per channel, equivalent to 84 MeV [2].

5.2. Event selection

As a measure of the response of cosmic ray muons to an individual calorimeter cell the most probable value (MOP) of the observed signal distribution after calibration using the UNO signal is used. This value is called the μ/UNO value defined as

$$\mu/\text{UNO}[\text{pC}] \equiv \left\{ Q_{\mu}[\text{pC}] \frac{I_{\text{UNO}}^{\text{nom}}[\text{nA}]}{I_{\text{UNO}}[\text{nA}]} \right\}_{\text{MOP}},$$

where $I_{\text{UNO}}^{\text{nom}}/I_{\text{UNO}}$ is the ratio of the nominal current from the uranium signal (see section 4) to the measured uranium current. The cell to cell variation of μ/UNO expresses the relative calibration uncertainty for muons of individual calorimeter cells when calibrated with the UNO signal.

Single muon events were selected by the following selection criteria. For muons in the HAC cells 93% of the signal had to be contained in one single cell. The corresponding number is 85% for the EMC cells. To assure that the particle is well contained in the center of a cell a cut on the relative difference of the left and right (L–R) photomultiplier signal was used. In order to avoid low energy tails, a minimum signal in the hit cell was demanded. Furthermore events without a sig-

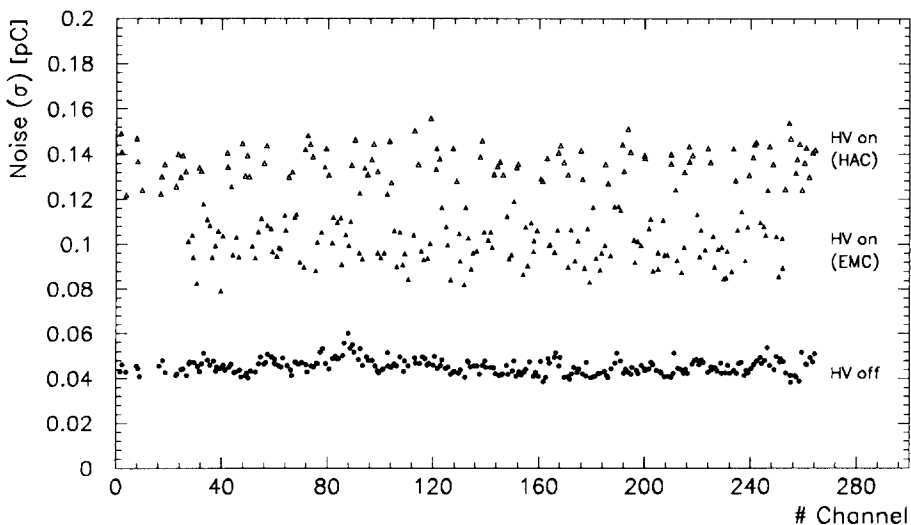


Fig. 5. Noise of the high gain channels of a typical module.

nificant charge in another longitudinal section were rejected. The fraction of triggers retained are $43 \pm 7\%$ for FEMC, $41 \pm 3\%$ for FHAC, $60 \pm 9\%$ for REMC and $43 \pm 2\%$ for RHAC. An overview of the cuts is given in Table 1.

To study the influence of the selection criteria on the results of the calorimeter calibration the different cut values were varied within broad limits. The considered quantities for checking the effect were the mean value of the μ/UNO -distribution for a specific module, called $\langle \mu/\text{UNO} \rangle$, and its spread, called $\sigma(\mu/\text{UNO})$. Even for extreme values for the selection criteria the relative values $\sigma(\mu/\text{UNO})$ show changes of 0.1% or smaller, the absolute values $\langle \mu/\text{UNO} \rangle$ vary only at the 1% level. On this basis the systematic errors of the analysis for the relative calibration of the different calorimeter cells is estimated to be about 0.1%. The systematic effect on the absolute results is taken to be 0.6%.

A second independent analysis, using a different set of cuts, was performed for the EMC cells. The cuts were determined by looking at the energy deposit in the EMC cell where the bulk of the muon energy is contained (central cell) and the neighbouring cells. 80% of the energy must be contained in the central cell. The neighbouring cell with less energy must have an absolute signal less than 0.17 pC. A (L–R) cut of 1.7 pC was applied. A minimum energy deposit of 1.25 (2.5) pC was demanded for EMC (HAC) cells. Furthermore, for FCAL modules, it was required that 80% of the energy deposited in the HAC cell must be contained in the cell with the larger signal. For RCAL modules most of the energy must be deposited in one supertower. For these sample of cuts the fraction of retained triggers is $40 \pm 5\%$ ($30 \pm 5\%$) for FEMC (REMC).

5.3. Determination of μ/UNO

The sum of the left and right photomultiplier was used as the charge of a particular cell. In 2% of all cells only one side was available due to faulty photo-

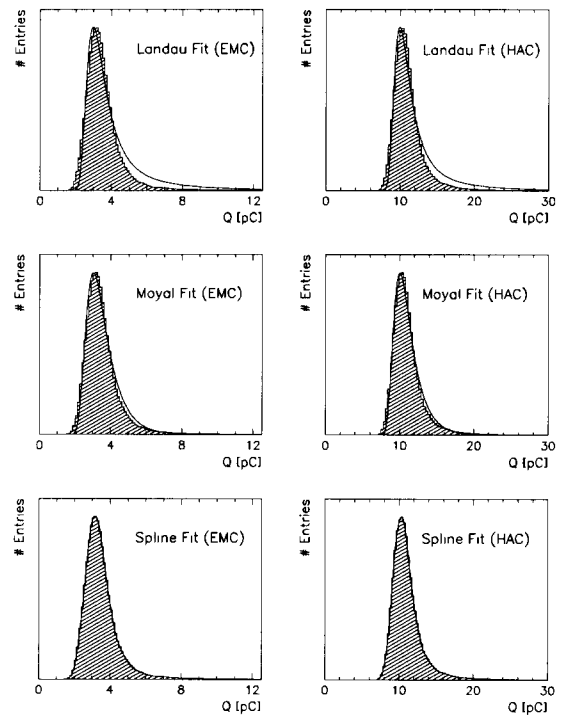


Fig. 6. High statistics samples of a typical FCAL module with different fit functions.

multipliers or problems with the readout electronics. In these cases twice the charge of the available phototube was used as the signal of the cell. The deposited charge of the muon was calculated by adding the signal deposited in the hit cell and its two neighbours.

As a first attempt to describe the data, Moyal and Landau functions [19,15] were used. The high statistic sample, obtained by adding all cells of a module, show that the data are poorly described by these functions (see Fig. 6). Therefore a cubic spline interpolation method was used for each module to parametrize the measured distribution. The algorithm is described in ref. [22].

Table 1
Cut values used during analysis

Cut type	FEMC	FHAC	REMC	RHAC
	Cut Set 1			
Signal fraction in hit cell	85%	93%	85%	93%
(L–R) cut	25%	25%	25%	25%
Minimum signal cut	1.92 pC	7.5 pC	1.92 pC	7.5 pC
Minimum charge in other longitudinal section	$Q_{HI} > 6.5 \text{ pC}$	$Q_{HI/2} > 6.5 \text{ pC}$	$Q_{HI} > 6.5 \text{ pC}$	$Q_{EM} > 1.5 \text{ pC}$
Fraction of retained triggers	$43 \pm 7\%$	$41 \pm 3\%$	$60 \pm 9\%$	$43 \pm 2\%$

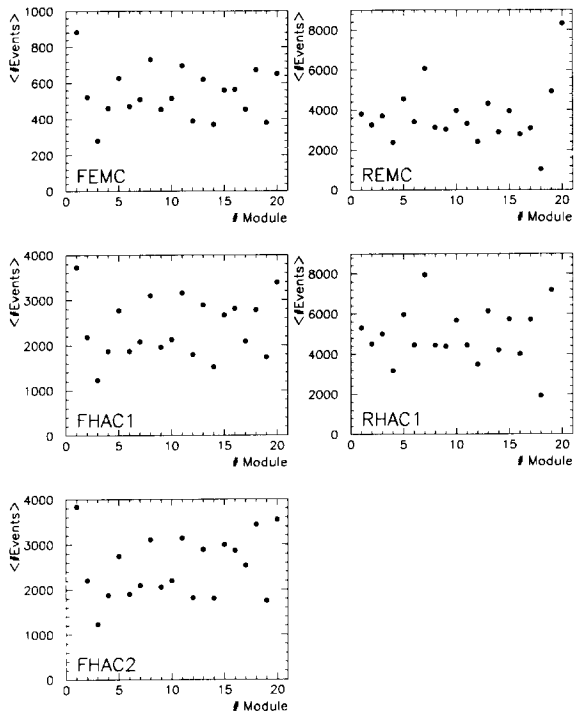


Fig. 7. Mean number of muons per cell versus module number.

The function, by construction, fits the distribution perfectly (see again Fig. 6). This parametrisation was used for fitting the distributions of the individual cells to obtain the most probable value which was then called the μ /UNO value as defined in section 5.2. As the second fit parameter the scale parameter of the y-axis was used.

6. Results

The average number of events per cell for each module that pass the cuts is shown in Fig. 7. The module number is given by the testing order. There is a significant difference between the FEMC and the other longitudinal sections. The smaller statistics for FEMC cells is a consequence of the $5 \times 20 \text{ cm}^2$ area instead of $20 \times 20 \text{ cm}^2$ for the HAC cells.

In Fig. 8 we present charge spectra for a typical cell of F/REMC, F/RHAC1 and FHAC2. The solid lines represent the result of a fit using the function determined via spline interpolation (see section 5.3). Fig. 9 shows μ /UNO as a function of the cell number for a typical FCAL module. The solid lines are the $\pm 1\%$ deviations from the mean value of μ /UNO for that module. The spread of μ /UNO for FEMC is bigger than for FHAC1/2 cells where the values are less than 1%.

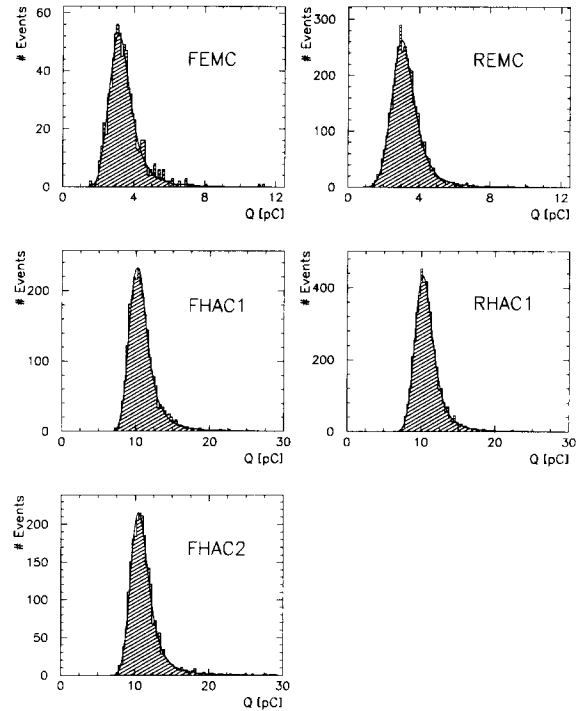


Fig. 8. Typical muon distributions for different longitudinal sections.

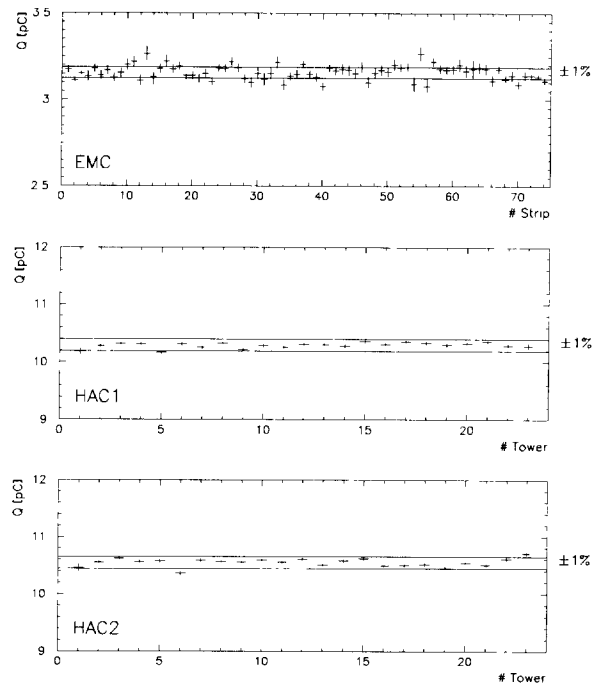


Fig. 9. μ /UNO for all FEMC, FHAC1 and FHAC2 cells of a typical module.

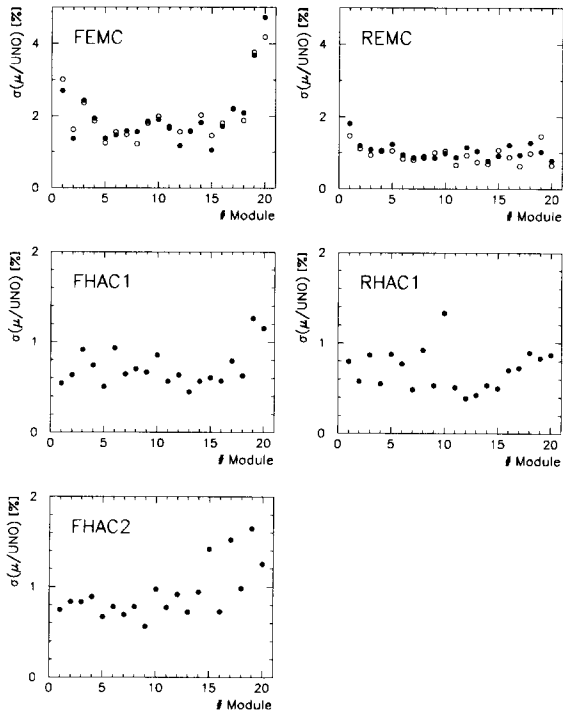


Fig. 10. $\sigma(\mu/UNO)$ for different longitudinal sections versus module number (dots: main analysis; open circles: second analysis for EMC cells).

The spread for all cells of one module is defined as:

$$\sigma(\mu/UNO) \equiv 100 \frac{\text{rms}}{\langle \mu/UNO \rangle} [\%],$$

where $\langle \mu/UNO \rangle$ is the mean value and rms the root mean square of the μ/UNO distribution. In Fig. 10 we plot the $\sigma(\mu/UNO)$ as a function of the module number. The black dots are the results of the main analysis. For F/REMC cells the results of the second analysis are overlayed using open circles. Both results are in good agreement. The mean difference is 0.2% which is compatible with the systematic errors estimated in section 5.

The $\sigma(\mu/UNO)$ averaged over all the modules, called $\overline{\sigma(\mu/UNO)}$, including the statistical error, the statistical error itself and the corrected quantity are given for the different longitudinal sections in Table 2. Whereas the values for F/RHAC are 0.9% or smaller, the F/REMC cells show results of 1.6% and 1.0% respectively. From Fig. 10 one can also see that the two last FCAL modules tested tend to have a bigger spread than the average. These modules are the special half sized modules to be mounted in ZEUS above and below the beampipe. The reason for this behaviour is not understood.

Up to now only cell to cell variations in single modules have been discussed. The variations between different modules can be studied using the quantity $\Delta(\mu/UNO)$:

$$\Delta(\mu/UNO) \equiv 100 \frac{\langle \mu/UNO \rangle - \overline{\langle \mu/UNO \rangle}}{\overline{\langle \mu/UNO \rangle}} [\%],$$

where $\overline{\langle \mu/UNO \rangle}$ is the mean value of $\langle \mu/UNO \rangle$ for all tested modules, also shown in Table 2. $\Delta(\mu/UNO)$ as a function of the module number is presented in Fig. 11 for the different longitudinal sections. The results from the second analysis are plotted in the same figure as open circles. Both results are again in good agreement. The mean difference is 0.6%, again compatible with the derived systematic errors. The Δ values are at the $\pm 1\%$ level for FCAL cells, but for RCAL one observes numbers of about $\pm 2\%$.

The μ/UNO distributions for all tested cells of the calorimeter are displayed in Fig. 12 for the different longitudinal sections. These distributions are, to a good approximation, Gaussian (a Gaussian fit is overlayed). The fitted means of the MOP values of all cells, called $\langle \mu/UNO \rangle_{ac}$, for the different longitudinal sections of F/RCAL are shown in Table 3.

The sigma from the Gaussian fit including statistical errors and the corrected value, called $\sigma \langle \mu/UNO \rangle_{ac}$, are also given in Table 3. These values represent the measured uncertainty in energy scale for a muon in the ZEUS calorimeter if calibrated with the UNO signal. The results obtained at CERN with 100 GeV muons

Table 2
Mean values of $\langle \mu/UNO \rangle$ and $\overline{\sigma(\mu/UNO)}$ averaged over all modules for different longitudinal sections

Section	$\langle \mu/UNO \rangle$ [pC]	$\overline{\sigma(\mu/UNO)}$ [%]	(stat. error) [%]	$\overline{\sigma(\mu/UNO)}$ (stat. error subtracted) [%]
FEMC	3.13	1.9	1.0	1.6
REMC	3.11	1.1	0.3	1.0
FHAC1	10.28	0.7	0.3	0.6
RHAC1	10.38	0.8	0.2	0.7
FHAC2	10.38	0.9	0.3	0.9

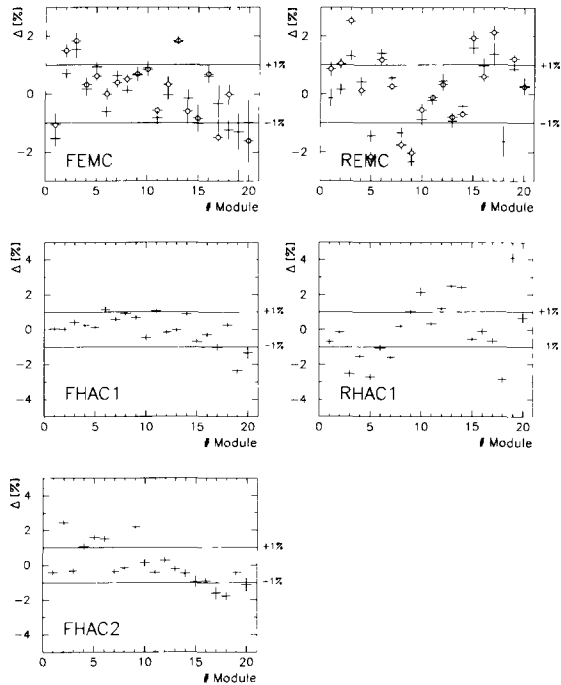


Fig. 11. $\Delta(\mu/UNO)$ for different longitudinal sections versus module number (crosses: main analysis; open circles: second analysis for EMC cells).

are also given in Table 3. Both sets agree within 0.4%, except for the RCAL cells. This difference is caused by the bigger module to module spread in the RCAL which had not been seen from the CERN calibration due to the small sample of tested modules.

For those modules also tested with beam muons, we compare $\Delta(\mu/UNO)$ in Fig. 13. The black dots show these result of the cosmic ray test and the crosses the results obtained using 100 GeV muons from the test beam. Both sets of data agree within 0.5%, except one RCAL module. The deviation of this module is not understood. Probably its handling between the CERN

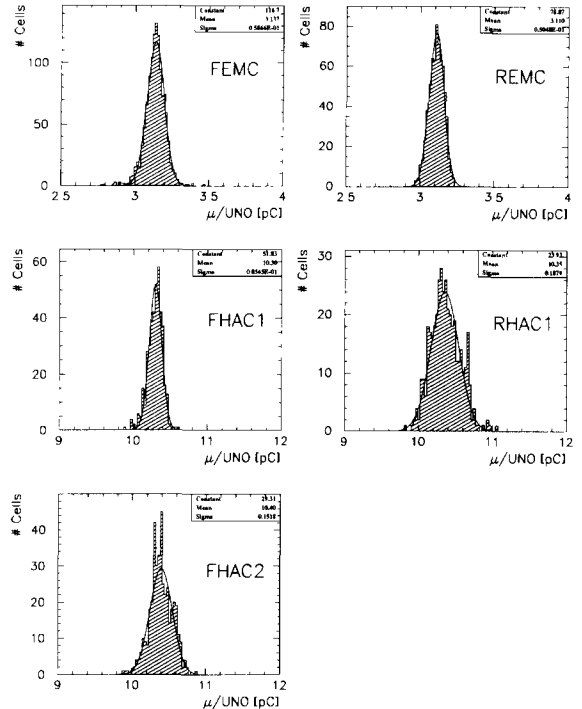


Fig. 12. μ/UNO distributions for different longitudinal sections.

calibration and cosmic ray tests is responsible for this effect.

In ref. [2] ratios of the mean values of different longitudinal sections are given. To be able to compare these results with the cosmic ray calibration a correction has to be applied to $\langle\mu/UNO\rangle_{ac}$ which takes into account the fact that the muons usually do not cross the tower perpendicular to the layer structure, as it was the case for the beam tests. Simple geometrical considerations of the mean crossing angle show that as example for REMC this correction amounts to 2.8%. In Table 4, besides the $\langle\mu/UNO\rangle_{ac}$ result from Table 3, the correction and the corrected result, called $\langle\mu/UNO\rangle_{ac,corr}$ are given. The ratios of the mean

Table 3
Mean values of μ/UNO and their width of all measured cells for different longitudinal sections

Section	$\langle\mu/UNO\rangle_{ac}$ (all cells) [pC]	$\sigma\langle\mu/UNO\rangle_{ac}$ (all cells) [%]	$\sigma\langle\mu/UNO\rangle_{ac}$ (stat. error subtr.) [%]	$\sigma\langle\mu/UNO\rangle$ (CERN) [%]
FEMC	3.14	1.9	1.6	1.2
REMC	3.11	1.8	1.8	1.0
FHAC1	10.30	0.8	0.8	0.9
RHAC1	10.36	1.8	1.8	0.7
FHAC2	10.40	1.5	1.4	1.1

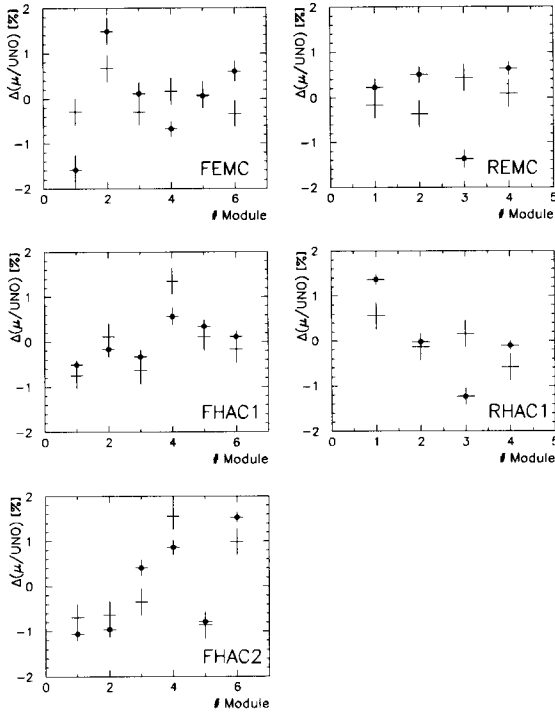


Fig. 13. Comparison of $\Delta(\mu/UNO)$ values obtained in the CERN beam test (crosses) and in the cosmic test (dots).

values for different longitudinal sections from cosmic ray muons and their statistical errors therefore are:

$$\frac{\langle \mu/UNO \rangle_{FEMC}}{\langle \mu/UNO \rangle_{REMC}} = 1.031 \pm 0.001 \quad (1.022) \quad [0.9\%],$$

$$\frac{\langle \mu/UNO \rangle_{FHAC1}}{\langle \mu/UNO \rangle_{RHAC1}} = 0.994 \pm 0.001 \quad (0.996) \quad [0.2\%],$$

$$\frac{\langle \mu/UNO \rangle_{FHAC2}}{\langle \mu/UNO \rangle_{FHAC1}} = 1.010 \pm 0.001 \quad (1.005) \quad [0.5\%],$$

$$\frac{\langle \mu/UNO \rangle_{FHAC1}}{\langle \mu/UNO \rangle_{FEMC}} = 3.262 \pm 0.001 \quad (3.283) \quad [0.6\%],$$

$$\frac{\langle \mu/UNO \rangle_{RHAC1}}{\langle \mu/UNO \rangle_{REMC}} = 3.383 \pm 0.001 \quad (3.366) \quad [0.5\%].$$

Table 4
Correction of the $\langle \mu/UNO \rangle_{ac}$ values for track length effects

Section	$\langle \mu/UNO \rangle_{ac}$ [pC]	Track length correction [%]	$\langle \mu/UNO \rangle_{ac,corr}$ [pC]
FEMC	3.14	-0.6	3.12
REMC	3.11	-2.8	3.02
FHAC1	10.30	-1.2	10.17
RHAC1	10.36	-1.2	10.23
FHAC2	10.40	-1.2	10.27

The results obtained at CERN with 100 GeV muons [2] are shown in round brackets. Additionally the relative differences of the two data sets are given in square brackets. The agreement is better than 0.6% which is compatible with the given systematic errors; solely the ratios of the EMC cells show a difference of 0.9%.

The results show that a calibration of the calorimeter using cosmic ray muons gives a comparable calibration precision as that using test beam muons.

More detailed information about the cosmic ray test of F/RCAL modules and further related studies can be found in refs. [13,11].

7. Conclusions

In this note the calibration of the ZEUS forward and rear calorimeter modules using cosmic ray muons was discussed. The cosmic ray test setup was described and the results were presented. The main results of this test are summarized below.

Cosmic ray muons can be used as a precision calibration method ($< 0.5\%$ as seen from the comparison between CERN and DESY results) for the ZEUS calorimeter.

Cosmic rays muons show that tower to tower and module to module calibration at the 1% level has been reached using the signal of the uranium radioactivity for normalisation.

Using cosmic ray muons, the calibration with the uranium signal could be checked for all modules of the ZEUS forward and rear calorimeter to a precision of about 0.5%. It would have been a prohibitive effort to bring all modules to a test beam.

The results demonstrate that an equally precise relative calibration can be obtained with cosmic muons as with beam muons. In ref. [2] it was demonstrated that the muon calibration tracks the calibration with electrons and hadrons within 1.0% for the electromagnetic and 0.9% for the hadronic section. Thus the cosmic muons also provide a precise calibration for showering particles for the ZEUS calorimeter.

Acknowledgements

We would like to thank all the people who made the cosmic ray test of the forward and rear calorimeter at DESY possible.

We gratefully acknowledge K. Dierks, G. Drews, L. Hervás, H. Kammerlocher, A. Odian, M. Rohde, F. Selonke, J. Straver and W. Vogel for their assistance in providing the setup of the experiment. We are also grateful to C. Farrow and many other people for their enthusiastic efforts in preparing the modules for operation. It is a pleasure to thank J. Hauschildt and K.

Löffler for technical support and the crane crew of hall II at DESY for their continuous effort in moving the modules in and out of the test stand. Finally, we thank R. Klanner, U. Kötz and H. Tiecke for their strong support and continuous interest.

References

- [1] A. Andresen et al., Nucl. Instr. and Meth. A 290 (1990) 95.
- [2] A. Andresen et al., Nucl. Instr. and Meth. A 309 (1991) 101.
- [3] A. Bamberger et al., The Laser/LED System of the FCAL/RCAL. ZEUS Note 90-119.
- [4] U. Behrens et al., Nucl. Instr. and Meth. A 289 (1990) 115.
- [5] U. Behrens et al., DESY 92-064 (1992).
- [6] Blankers et al., NIKHEF-H/90-11.
- [7] H. Boterenbrood et al., ZEUS Note 90-010; L.W. Wiggers and J.C. Vermeulen, Comp. Phys. Commun. 57 (1989) 316.
- [8] R. Brun and J. Zoll, ZEBRA User's Guide, CERN Computer centre, Program library, long write-up Q100.
- [9] R. Brun et al., PAW Physics Analysis Workstation, CERN Computer centre, Program library, long write-up Q121.
- [10] A. Caldwell, ZEUS internal note (1989).
- [11] G. Cases, Ph.D. thesis, Universidad Autónoma de Madrid, 1992. (The absolute μ /UNO values that appear in that manuscript are 20% too high due to a global error in the electronic calibration constants.)
- [12] E. Daubie et al., Nucl. Instr. and Meth. A 252 (1986) 435.
- [13] A. Fürtjes, Ph.D. thesis, Universität Hamburg, 1993, DESY F35D-1993-032.
- [14] T. Ishii et al., Nucl. Instr. and Meth. A 320 (1992) 449.
- [15] L. Landau, J. Phys. 8 (1944) 201.
- [16] J. Mitchell et al., ZEUS Note 90-104.
- [17] J. Möschen, Diploma thesis, Universität GH Duisburg (1987), ZEUS Note 87-006.
- [18] K. Molthagen, Diploma thesis, Universität Hamburg (1991).
- [19] J. Moyal, Philos. Mag. 46 (1955) 263.
- [20] D. Notz, ZEUS Note 90-126, 90-126a.
- [21] Particle Data Group, Phys. Lett. B 239 (1990).
- [22] W.H. Press, B.P. Flannery, S.A. Teukolsky and W.T. Vetterling, Numerical Recipes: The Art of Scientific Computing (Cambridge Univ. Press).
- [23] B. Rossi, Rev. Mod. Phys. 20 (1948) 237.
- [24] W. Sippach et al., IEEE Trans. Nucl. Sci. NS-36 (1989) 465; A. Caldwell et al., Nucl. Instr. and Meth. A 321 (1992) 356. L. Hervás, Ph.D. Thesis, DESY Internal Report F35D-91-01 (1991), FTUAM-EP/90-02.
- [25] J. Straver, ZEUS-Note 89-123.
- [26] J. Straver, Ph.D. Thesis, NIKHEF, Netherlands (1991).
- [27] P. Vande Vyvre, The MODEL Buffer Manager Users's Guide, CERN Computer centre, Program library.
- [28] ZEUS Collaboration. ZEUS, A Detector for HERA, Letter of Intent, DESY (1985); The ZEUS Detector, Technical Proposal, DESY (1986); The ZEUS Detector, Status Report 1987, DESY (1987); The ZEUS Detector, Status Report 1989, DESY (1989); The ZEUS Detector, Status Report 1993, DESY (1993)